



Performance of a detonation driven shock tunnel

Jiwei Li¹, Yingxin Tan²

School of Chemical and Environmental Engineering, North University of China, Taiyuan, China, 030051

Qiu Wang³, Wei Zhao⁴, Pan Lu⁵,

State Key Laboratory of High Temperature Gas Dynamics, Institute of Mechanics, Chinese Academy of Sciences, Beijing, China, 100190

Because of the high costs of flight tests, ground test facilities are a necessity in hypersonic flow research. Compared with other impulse facilities, shock tunnels show their advantages in relatively large-size models and low operational costs. To continuously improve the capacities of shock tunnels, a new detonation-driven shock tunnel was developed in the Laboratory of High Temperature Gas Dynamics (LHD), Institute of Mechanics, Chinese Academy of Sciences. In this paper, performance of the detonation-driven shock tube is investigated, with the help of numerical calculation. Some key issues, including the filling of the gases, pressure loss caused by diaphragm rupture, and the nearly tailored status are discussed in detail.

Nomenclature

ρ	=	density, kg/m ³
u	=	velocity, m/s
e	=	total energy, J
P	=	pressure, Pa
M	=	molecular weight, g/mol
γ	=	specific heat ratio
T	=	temperature, K
R_0	=	universal gas constant
Ms	=	Mach number of shock wave
a	=	sound velocity, m/s

I. Introduction

Hypersonic technology is one of the most important research frontiers for aerospace program. Unlike what is seen by vehicles in subsonic or supersonic flights, hypersonic vehicles encounter an aero-thermodynamic environment characterized by strong shocks and high temperatures, that are accompanied by the vibrational excitation, dissociation and even the ionization of gas molecules. These complex phenomena make it difficult for an accurate prediction of the aerodynamic environment around a particular vehicle, and it is also an important issue in the area of gas dynamics research[1], which needs in-depth investigation. Although research in hypersonic technology has made great progress with the development of theories and numerical computation methods for decades, the ground test is still the main means of hypersonic research.

In order to meet the requirements as determined by ground experiments of hypersonic vehicles, advanced hypersonic test facilities have been under development for more than 50 years[2]. A air-heated, combustion-heated,

¹ Student, School of Chemical and Environmental Engineering, North University of China, No.3 XueYuan road, 1306532444@qq.com

² Professor, School of Chemical and Environmental Engineering, North University of China, No.3 XueYuan Road, 13934240901@163.com

³ Assistant Professor, State Key Laboratory of High Temperature Gas Dynamics, No.15 Beisihuanxi Road, wangqiu@imech.ac.cn

⁴ Professor, State Key Laboratory of High Temperature Gas Dynamics, No.15 Beisihuanxi Road, zw@imech.ac.cn

⁵ Student, State Key Laboratory of High Temperature Gas Dynamics, No.15 Beisihuanxi Road, lupan@imech.ac.cn

and arc-heated hypersonic wind tunnels have been developed, as have heated-light-gas-driven, free-piston-driven and detonation-driven shock tunnels. Taking account of real gas effects on hypersonic flows and high enthalpy requirements, the shock tunnel would be the most promising facility to provide hypersonic test flows. But, a shock tunnel must incorporate a high performance driver due to the huge energy requirement. Among the existing driving techniques, the detonation drivers are capable of producing high enthalpy and high pressure test flows simultaneously with easy operation and low capital investment. The detonation-driven method was first proposed to solve this problem by Bird in 1957[3]. A detonation-driven shock tube was first designed and installed by Yu[4] [5]. The TH2 that operated in a backward-running mode was developed in Aachen, Germany[6]. Later, a larger detonation-driven shock tunnel named HYPULSE was installed in GASL, USA[2]. These detonation-driven shock tunnels can be operated to provide either stable test flows with a long driving time at a relatively low enthalpy level or high-enthalpy flows with a short test duration. Recent rapid progress shows that detonation-driven hypersonic test facilities represent a promising method for implementing hypersonic vehicle ground tests.

But, no single ground test facility can fully simulate the many aspects of hypersonic flight. The quality of the free-stream flow, Mach number, Reynolds number at altitude, and gas chemistry cannot be controlled simultaneously in any single facility, if at all. Nearly every tunnel suffers from various problems, each having unique advantages and disadvantages. In order to promote the fundamental study of aero-thermo-dynamics and engineering applications in hypersonic flight, it is necessary to extend and supplement the capabilities of existing detonation driven shock tunnels. Nowadays, a new detonation-driven shock tunnel named JF-X was developed at LHD. As described in this paper, preliminary experiments, associated with numerical simulation, were carried out to investigate several key problems which impact the performance of the JF-X shock tunnel. Firstly, a critical nozzle was designed to control the rate of filling of gas and shock tube conditions that extended the test duration were analyzed. Then, the pressure loss caused by the diaphragm rupturing was also investigated.

II. Facility

For a detonation shock tunnel, two modes of operation are usually used. The mode in which the ignition position is located at the end of driver section is called the forward-running mode. This mode is, usually used to generate high enthalpy flow. The other mode, in which the ignition is performed near the diaphragm, is called the backward-running mode, and was the mode selected in the new tunnel because of, its stable performance after detonation. The detonation wave is initiated near the main diaphragm, and propagates upstream of the driver section. Meanwhile, the reactive high pressure and high temperature gas behind the detonation would rupture the main diaphragm, and generate a strong incident shock, which propagates through the driven tube, producing the interface (contact surface) between the driver and driven gases. When the primary shock strikes the end of the driven section, it is reflected, generating a reservoir region of almost stationary, high pressure and heated air [7]. Based on these techniques, several detonation-driven shock tunnels have been developed in the State Key Laboratory of High Temperature Gas Dynamics (LHD), Institute of Mechanics, Chinese Academy of Sciences (CAS), the high-enthalpy shock tunnel (JF10), the long-test-duration hypervelocity shock tunnel (JF12)[8] and the high-enthalpy expansion tunnel(JF16). These shock tunnels can provide hypersonic flows of higher total temperature than JF8A, which uses the high pressure air as the drive source. Among these are, the improved JF10 shock tunnel extends the effective test time to more than 6ms and provides conditions to conduct testing when the total temperature is about 10000K. The JF12 shock tunnel is capable of reproducing flight conditions at altitude of 25 to 50 Km and of that covering the Mach numbers from 5 to 9 with a test duration of more than 100 ms, and it has the ability to test full-sized or nearly full-sized hypersonic vehicles. The JF 16 expansion tunnel can generate a test flow of over 8300m/s and a total enthalpy up to 40MJ/Kg, with test durations being around 50 to 100ms. To extend and supplement the capacities of existing shock tunnels, with the main parameters shown in Table 1, a new detonation driven shock tunnel, named JF-X, was developed at LHD. A photo of the shock tunnel is shown in Figure 1. It is, a reflected shock tunnel, with the driver section made with 42CrMo steel under the maximum allowable pressure of 50 MPa, and the driven section with SUS304 stainless steel under a pressure of 30 MPa. Other parameters can also be found in Table 1. Several pressure transducers were mounted to measure the velocity and pressure in the shock tube.

JF-X shock tunnel operates with backward-running mode which has been studied in LHD [9]. To explain the principle of the backward-running mode, the wave diagram of the detonation shock tube is shown in Figure 2. The detonation wave is initiated near the main diaphragm and propagates leftward to the dump section. A Taylor expansion wave follows the detonation wave. Meanwhile, the high-temperature and high-pressure detonated product gas that remains in the driving section acts as the driver source for the shock tube. After the main diaphragm rupture, an incident shock wave propagates almost simultaneously rightward in the shock tube followed by the interface. It is reflected at the shock tube end wall as shown in figure 2. If the reflected shock wave crosses over the interface

without any reflected wave, that is the ideal experimental condition expected. In this paper, the simulations don't contain the dump section or the nozzle.

Table 1 Facility comparison

Facility	JF8A	JF10	JF12	JF-X
Driver section	11 m in length 150 mm in diameter	10 m in length 150 mm in diameter	99 m in length 400 mm in diameter	6.5 m in length 126 mm in diameter
Shock tube	21 m in length 155 mm in diameter	12.5 m in length 100 mm in diameter	89 m in length 720 mm in diameter	6.6 m in length 126 mm in diameter
Operation mode	High pressure Air Contoured	Forward detonation Conical	Backward detonation Contoured	Backward detonation Contoured
Nozzle	5 m in length 0.8 m in exit diameter	2 m in length 0.5 m in exit diameter	15 m in length 2.5 m in exit diameter	2.3 m in length 0.5 m in diameter
Temperature T_0	~1100 K	~10000 K	~3500 K	~7000 K



Figure 1. Photo of JF-X detonation shock tunnel

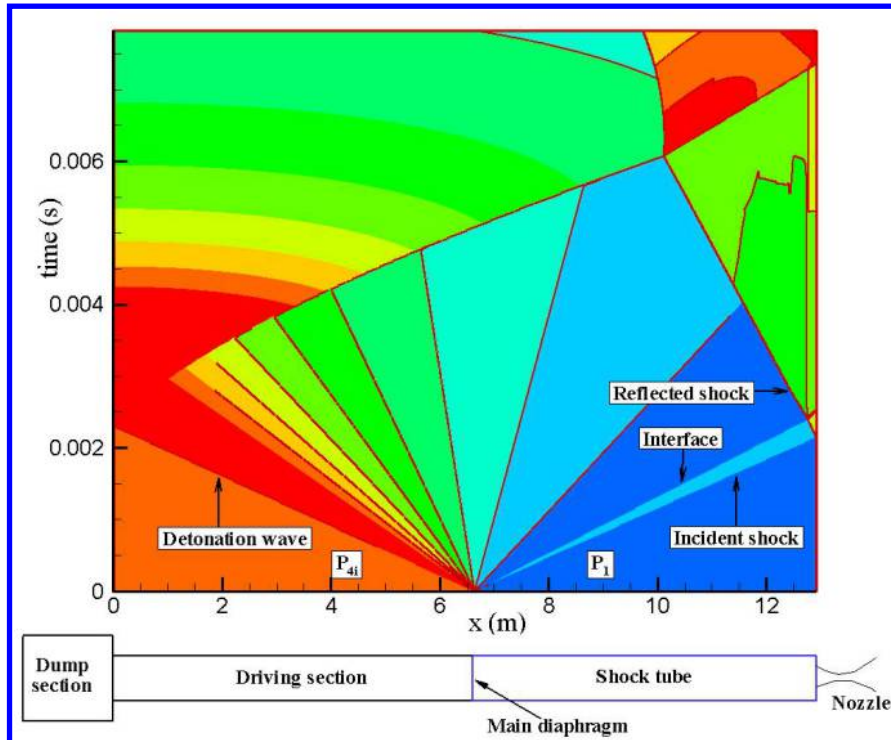


Figure 2. Schematic of the detonation driven shock tube and wave diagram

III. Numerical simulations

To give a valuable complement to the experimental design and to better understand the wave process of the shock tube driven by detonation, numerical simulations were conducted for this paper. The shock tube involves detonation of the flammable mixtures in the detonation chamber and dissociation of the test gas (air in the paper) in the shock tube, which are rather complicated processes. Modeling all phenomena in detail is unrealistic. Also, the viscous term, heat conduction and rupture process of the diaphragm are neglected.

The numerical method is based on a one-dimensional chemical nonequilibrium flow model, with the equations, written in conservation form,

$$A \frac{\partial U}{\partial t} + \frac{\partial AF(U)}{\partial x} - \frac{\partial A}{\partial x} H - S_c = 0 \quad (1)$$

where the state vector $U = (\rho_i, \rho, \rho u, e, \rho \alpha, \rho \beta)^T$, the flux vector $F = (\rho_i u, \rho u, \rho u^2 + p, (e + p)u, \rho \alpha u, \rho \beta u)^T$, the chemical reaction source term $S_c = (\dot{\omega}_i, 0, 0, 0, \dot{\omega}_\alpha, \dot{\omega}_\beta)$, and the wall pressure source term $H = (0, 0, p, 0, 0, 0)^T$, where ρ , u , e , p , and A are the density, velocity, total energy, and pressure of gas, and cross-sectional area, respectively. The subscript “ i ” denotes the species (O_2 , N_2 , O , N). α and β are the process parameters of the chemical induction and the chemical transformation, respectively; ω_α and ω_β are the rates of the chemical induction and the chemical transformation, respectively; and ω_i is the chemical source term for species i .

For the detonation process, a two-step chemical reaction model is used and ρ_i is set to 0 in the computation. For the details of this model, please refer to reference [10]. Additional, the finite-rate chemistry developed by Park [11] is used for air in the shock tube without ionization, considering five components, O_2 , N_2 , O , N , and NO . Based on these chemical reaction models and the dispersion controlled dissipation scheme proposed by Jiang [12], a code has been developed and successfully applied to the simulations of a detonation-driven shock tube [13].

IV. Some results and discussion

A. Filling of the gases

The filling and mixing of the gases for detonation has an important effect on the stability and repeatability of the driving performance. In order to insure the ratio of oxy-hydrogen mixture, calibrations should be carried out before experiments. The filling system consists of a critical nozzle, a valve and a pressure regulator, as shown in Figure 3. It is based on the principle that when the nozzle reaches the speed of sound in the throat, the mass flow rate will not be affected by the pressure downstream. Then the mass flow rate is calculated by the following equation,

$$m = \rho^* A^* a^* = P_0 \sqrt{\frac{\gamma M}{R_0 T_0}} \left(\frac{2}{\gamma + 1} \right)^{\frac{\gamma + 1}{2(\gamma - 1)}} A^* \quad (2)$$

where ρ^* , a^* , P_0 , γ , M , T_0 represent density, sound speed, filling pressure, specific heat ratio, molecular weight and temperature of the filling gas; A^* and R_0 are the area of the critical nozzle throat and the universal gas constant, respectively.

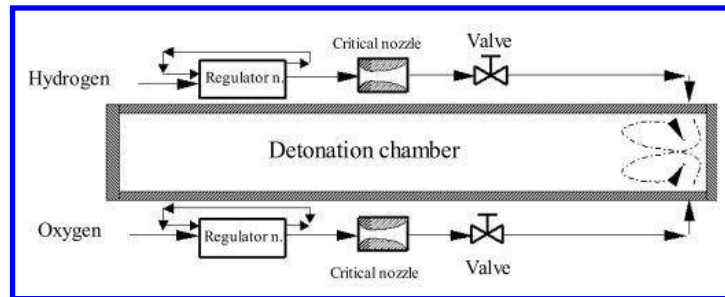


Figure 3. Illustration of filling and mixing oxy-hydrogen with critical nozzles

It is assumed that the ratio of the oxy-hydrogen mixture is n , that is

$$n = \frac{m_1/M_1}{m_2/M_2} \quad (3)$$

where subscripts “1” and “2” represent hydrogen and oxygen respectively. Substituting equation (2) into equation (3), we get:

$$n = \frac{(P_0)_1}{(P_0)_2} \times \sqrt{\frac{(T_0)_2}{(T_0)_1}} \times \frac{(A^*)_1}{(A^*)_2} \quad (4)$$

Since the total temperature of the two gases is at room temperature and essentially unchanged during the filling process, the effects of temperature on n are neglected here. Then,

$$n = 4 \frac{(P_0)_1}{(P_0)_2} \times \frac{(A^*)_1}{(A^*)_2} \quad (5)$$

When A^* is confirmed, it is easy to get a different value n by changing P_0 . Calibration of the hydrogen and oxygen systems is conducted with the results shown in Figure 4. Our target pressure in the driver section is 2.0 MPa with n close to 2. The filling pressures are kept constant, which here are 5.5 MPa for hydrogen and 4.1 MPa for oxygen, and much higher than the target pressure, in order to keep the velocity of sound at the critical nozzle throat. Monitoring the pressure changes in the driving tube, the filling rate and stability could be obtained, and are shown in Figure 4. During an exact experiment, the equivalence ratio of hydrogen and oxygen could be obtained during the filling process by monitoring the pressure changes of gas supply, as shown in Figure 5. The amount of hydrogen and oxygen in the driver section were increased linearly, and the ratio was almost constant during the entire filling process. The total experimental filling time was 397s, almost the same as that calculated through our calibration results, that was 395s. We can say that a needed initial gas condition in the driving tube could be exactly obtained by this filling system.

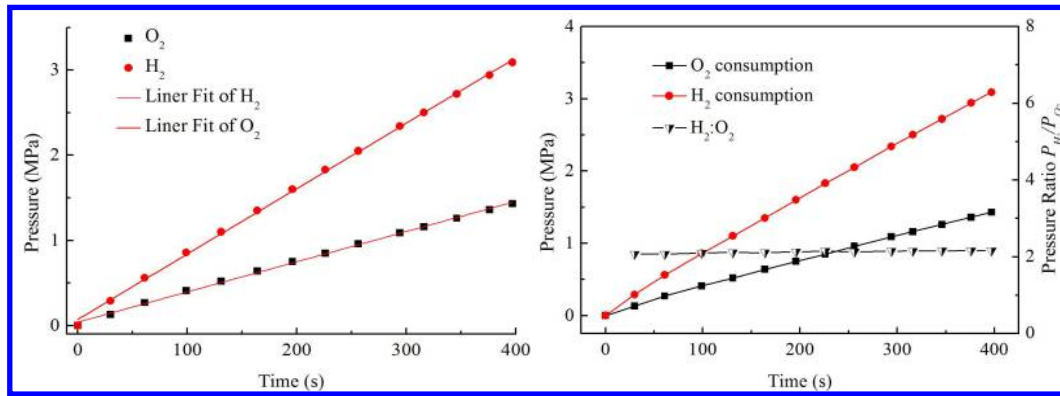


Figure 4. Fitting curve of filling process

Figure 5. Mixing ratio during filling process

B. Shock tube conditions

According to the definitions of conventional shock tunnel terminology, subscripts “4i” and “1” represent the initial condition of the driver section and the driven section respectively, subscript “4” represents the condition of detonation products. “ M_s ” represents the primary incident shock wave Mach-number in the shock tube and “ a ” is the local velocity of sound.

For a shock tunnel, effective test time is important. To lengthen the effective test time, it is expected that the reflected shock wave matches with the interface, which means that it crosses over the interface without any reflected wave. Then, a series of experiments were conducted to obtain a good performance of the facility, with the help of simulation. Test conditions are shown in Table 2.

Table 2 Initial conditions

	Driver Gas	Driven Gas
Species	H ₂ , O ₂	Air
Ratio	2.0	-
Pressure	P _{4i} =2MPa	P ₁ =20, 11.6, 15KPa

Figures 6 and 7 show the typical stagnation pressure histories at the end wall of the shock tube, including both experimental and numerical results. The results were obtained under the conditions of initial pressure $P_{4i}=2$ MPa, the equivalence ratio is 2 and with different P_1 . There was an obvious difference in the first 0.5 ms for the stagnation pressure, which then tended to the same value of almost 10 MPa for the three cases. The plateau pressure continued for more than 6 ms. The numerical results were slightly higher than the experimental results, which may be caused by the pressure loss while rupturing the metal diaphragm. Figure 8 shows the stagnation temperature histories of the numerical simulation. The results showed that the pressure of the driven section P_1 has a remarkable influence on the total temperature. It is About 6000K and stays constant for more than 6s while P_1 is 11.6KPa.

The driving capacity was considered to be strongly influenced by the rupturing condition of the diaphragm placed between the driver section and shock tube [14]. Using the shock tube theory, the pressure ratio of P_4 to P_1 can be calculated by the following equation.

$$\frac{P_4}{P_1} = \left[1 + \frac{2\gamma_1}{\gamma_1 + 1} (M_s^2 - 1) \right] \left[1 - \frac{\gamma_4 - 1}{\gamma_1 + 1} \times \frac{a_1}{a_4} \left(M_s - \frac{1}{M_s} \right) \right]^{\frac{2\gamma_4}{\gamma_4 - 1}} \quad (6)$$

With the detonation parameters obtained by a numerical calculation in section 2, together with M_s and P_1 , which could be accurately measured, it was easy to calculate P_4 , which is the pressure effective for driving the gas in the shock tube. Then, the pressure loss by rupture of the diaphragm could be calculated with this P_4 and the detonation pressure by CJ theory. Experimental results show that the pressure loss was about 30% for selected diaphragm when the initial gas pressure was 2MPa, with the mixing ratio of hydrogen and oxygen being 2.

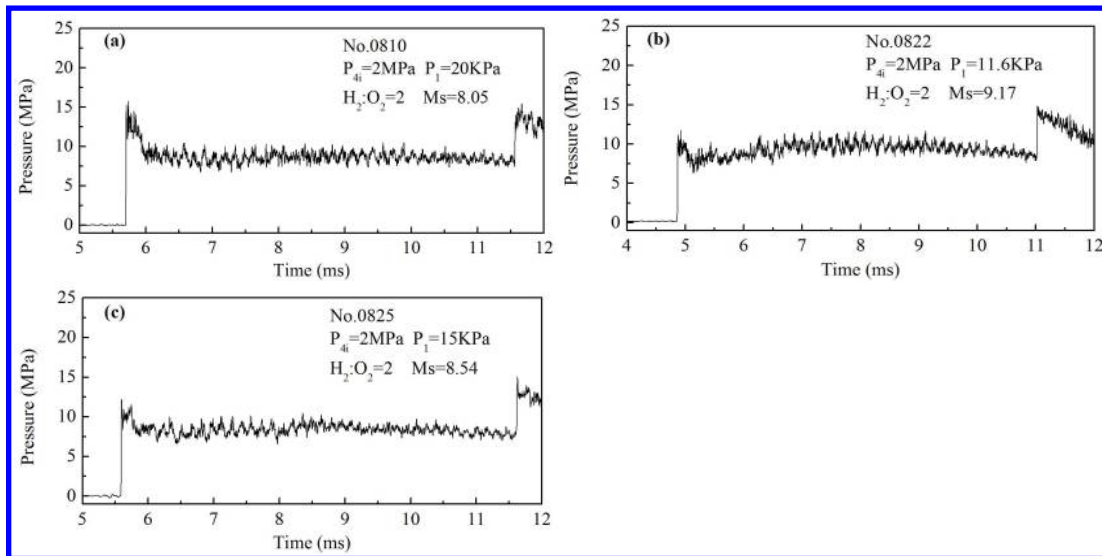


Figure 6. Stagnation pressure histories measured at the end wall of the driven section (a) $P_1=20$ kPa, (b) $P_1=11.6$ kPa, (c) $P_1=15$ kPa

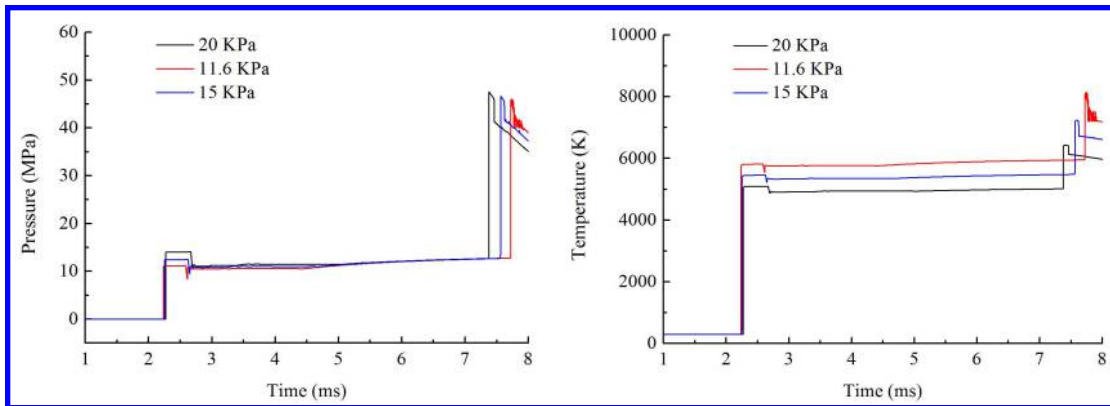


Figure 7. Simulated stagnation pressure histories under different values of P_1

Figure 8. Simulated stagnation temperature histories under different values of P_1

C. Pressure loss caused by diaphragm rupture

Figure 9 shows the relationship between Mach number of the shock wave M_s and the different pressures of the driven section, P_1 , under the condition for the initial pressure of the driver section, $P_{d1} = 2\text{MPa}$, and with the equivalence ratio being 2. The steel diaphragm was installed between the driver section and shock tube with an aggregate thickness of 3.4mm and the effective thickness of 0.65mm. The Mach number of shock wave decreased as the pressure P_1 increased. But the Mach number as estimated by numerical simulation is markedly higher than the experimental results. Possible reasons for the lower Mach number include the ideal assumptions of the diaphragm opening instantaneously and the rupture period of the diaphragm in the simulation program. To take into account the influence of the diaphragm, define the non-dimensional pressure ratio, P_4/P_{40} , of value P_4 as calculated by using the experimental M_s to the value P_{40} that is calculated by the simulation program. Figure 10 shows the relationship between P_4/P_{40} and the pressure of the shock tube, P_1 . The value of P_4/P_{40} decreased lightly with increases of the initial pressure in the shock tube, but the actual driving pressure calculated by experimental M_s is almost 70 percent of the pressure of that calculated by CJ theory.

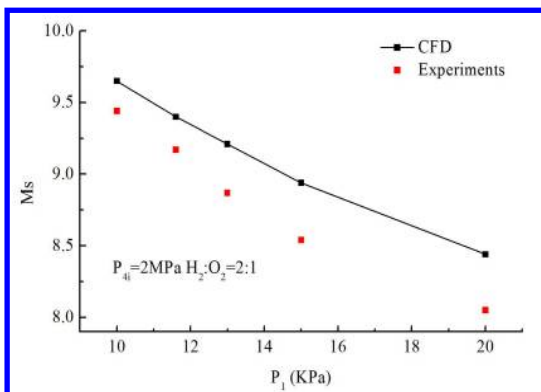


Figure 9. Relationship between Mach number of the shock wave M_s and the pressure of shock tube P_1

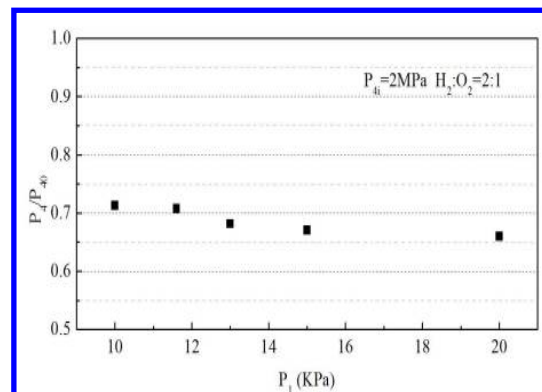


Figure 10. Relationship between pressure ratio P_4/P_{40} and the pressure of the shock tube, P_1

V. Conclusions

A new detonation-driven shock tunnel was designed and installed at LHD. Operating in the backward-running mode, preliminary experiments were set up to clarify the performance of the filling of the gases and shock tube conditions. The influence of pressure loss caused by rupture of the diaphragm was also investigated. The results are summarized as follows.

By using the critical nozzle, the ratio of aeration could be controlled precisely and maintained at nearly a constant rate during the entire process. That is precious for insuring data accuracy and repeatability of experiments.

In the backward-running mode, the effective test time is more than 5ms, sufficient to provide the high enthalpy and pressure airflow required. That is, the JF-X detonation driven shock tunnel has enough capability to promote the desired aerodynamics experiments.

The pressure loss caused by diaphragm rupture can not be neglected. For a specific diaphragm, a series of experiments should be launched to confirm the pressure loss under different initial conditions.

Acknowledgments

This work was supported by the National Natural Science Foundation of China (Grant Nos. 11402275, 11472280 and 11532014).

References

- ¹Bertin J J, Cummings R M., "Fifty years of hypersonics: where we've been, where we're going," *Progress in Aerospace Sciences*, Vol 39, No. 6-7, 2003, pp. 511-536.
- ²Lu, F. K., Marren, D. E., *Advanced Hypersonic Test Facility*, Progress in Astronautics and Aeronautics, Reston, 2002, p.198.
- ³Bird, G.A., A note on combustion driven tubes. Royal Aircraft Establishment, Vol 146, AGARD Report, May 1957
- ⁴Yu H R., Esser B., Lenartz M, Grönig, H., "Gaseous detonation driver for a shock tunnel," *Shock Waves*, Vol 2, No. 4, 1992, pp. 245-254.
- ⁵Yu, H. R., Chen, H., Zhao, W., "Advances in detonation driving techniques for a shock tube/tunnel," *Shock Waves*, Vol 15, No. 6, 2006, pp. 399-405.
- ⁶Vennemann, D., "Hypersonic test facilities available in Western Europe for aerodynamic/aerothermal and structure/material investigations," *Philosophical Transactions of the Royal Society A Mathematical Physical & Engineering Sciences*, Vol 357, No. 357, 1999, pp. 2227-2248.
- ⁷Zhao, W., Jiang, Z. L., Saito, T., Lin, J. M., Yu, H. R., Takayama, K., "Performance of a detonation driven shock tunnel," *Shock Waves*, Vol 14, No. 1, 2005, pp. 53-59.
- ⁸Jiang, Z. L., Li, J. P., Zhao, W., Liu, Y. F., Yu, H. R., "Investigating into techniques for extending the test-duration of detonation-driven shock tunnels," *Chinese Journal of Theoretical & Applied Mechanics*, Vol 44, No. 5, 2012, pp. 824-831.
- ⁹Yu, H. R., Zhao, W., "The use of oxy-hydrogen detonation driver for generation of high enthalpy flow," *20th International Symposium on Rarefied Gasdynamics*, Beijing, China, 1997, pp. 927-933
- ¹⁰Sichel M., Tonello, N. A., Oran, E. S., Jones, D. A., "A two-step kinetics model for numerical simulation of explosion and detonation in H₂-O₂ mixtures," *Proceedings of the Royal Society A Mathematical Physical and Engineering Sciences*, Vol 470, No. 2168, 2014, pp.49-82.
- ¹¹C. Park., "Review of chemical-kinetic problems of future NASA missions, I: earth entries," *Journal of Thermophysics and Heat Transfer*, Vol 7, No. 3, 1993, pp. 385-398.
- ¹²Jiang, Z. L., Takayama K., Chen, Y. S., "Dispersion conditions for non-oscillatory shock capturing schemes and its applications," *Computational Fluid Dynamics Journal*, Vol 4, No. 2, 1995, pp. 137-150.
- ¹³Li, J. P., Jiang, Z. L., Chen, H., "Numerical study on backward-forward double detonation driver for high-enthalpy shock tubes," *Chinese Journal of Theoretical and Applied Mechanics*, Vol 39, No. 3, 2007, pp. 343-349.
- ¹⁴Yamanaka, A., Ariga, Y., Obara, T., Cai, P., Ohyagi, S., "Study on Performance of Detonation-Driven Shock Tube," *JSME International Journal*, Vol 66, No. 45, 2000, pp.425-431.